Available online at www.sciencedirect.com

ScienceDirect

Ceramics International 40 (2014) 3333–3339

CERAMICS INTERNATIONAL

www.elsevier.com/locate/ceramint

Sintering behavior and microwave dielectric properties of a new low-permittivity ceramic system $Ca(Mg_{1-x}Al_x)(Si_{1-x/2}Al_{x/2})_2O_6$

Huanping Wang[a], Denghao Li[a], Qinghua Yang[a], Ruoshan Lei[a], Hongping Ma[b], Shiqing Xu[a,*]

[a]College of Materials Science and Engineering, China Jiliang University, Hangzhou 310018, PR China
[b]School of Mechanical & Automotive Engineering, Zhejiang University of Science and Technology, Hangzhou 310012, PR China

Received 6 August 2013; accepted 23 September 2013
Available online 29 September 2013

Abstract

The diopside ceramics with a formula of $Ca(Mg_{1-x}Al_x)(Si_{1-x/2}Al_{x/2})_2O_6$ ($x=0.01$–0.3) were synthesized via a traditional solid-state reaction method, and their solid solubility, sintering behavior and microwave dielectric properties were investigated. The results revealed that the solubility limit of Al_2O_3 in $Ca(Mg_{1-x}Al_x)(Si_{1-x/2}Al_{x/2})_2O_6$, which is defined as x, was between 0.15 and 0.2, and a second phase of $CaAl_2SiO_6$ presented when the x value reached 0.2. Appropriate Al^{3+} substitution for Mg^{2+} and Si^{4+} could promote the sintering process and lower the densification temperature, and a broadened densification temperature range of 1250–1300 °C was obtained for the compositions of $x=0.08$–0.15. With the increase of the x value, the dielectric constant (ε_r) increased roughly linearly, and the temperature coefficient of frequency (τ_f) showed a rising trend. The $Q\times f$ values increased from 57,322 GHz to 59,772 GHz as the x value increased from 0.01 to 0.08, and then they were saturated in the range of $x=0.08$–0.2. Further increase of the x value ($x\geq 0.25$) deteriorated the microwave dielectric properties. Good microwave dielectric properties of $\varepsilon_r=7.89$, $Q\times f=59{,}772$ GHz and $\tau_f=-42.12$ ppm/°C were obtained for the ceramics with the composition of $x=0.08$ sintered at 1275 °C.

Keywords: Microwave dielectric properties; Low-permittivity ceramic; $Ca(Mg,Al)(Si,Al)_2O_6$; Solubility limit

1. Introduction

The development of microwave dielectric resonators for application in wireless communication systems such as 3G cellular phones, direct broadcasting satellites, wireless local area networks and global positioning systems has been rapidly progressed in the past decade [1–4]. The available frequencies have therefore been extended from microwave to millimeter-wave ranges because large quantity of information can be transported with a high speed in the later range. A high operating frequency in these microwave applications requires dielectric materials with a low dielectric constant (ε_r), a high quality factor ($Q\times f$) and a zero temperature coefficient of resonant frequency (τ_f) [5–7]. Low permittivity can not only minimize the cross-coupling between conductors but also shorten the propagation delay time of electromagnetic signal. Furthermore, high quality factor can increase the frequency selectivity, while near-zero temperature coefficient of the resonant frequency can ensure the stability of the operating frequency against temperature fluctuations.

Several low-permittivity ceramic systems such as $Li_3AlB_2O_6$, Mg_2TiO_4, $(Mg, Zn)Al_2O_4$, MWO_4 (M=Mg, Zn, Ni, Co, Li, Ca, Te), $MMoO_4$ (M=Li, Zn, Ca, Al, In), $M_3(VO_4)_2$ (M=Mg, Ba, Ca, Bi), AMP_2O_7 (A=Ca, Sr; M=Zn, Cu) and $Y_2Ba(Cu, Mg)O_5$ have been investigated for microwave applications [7–22]. Moreover, $MSiO_3$ (M=Mg, Zn, Ca) ceramics have been proved to be excellent dielectric materials with low dielectric constant and low dielectric loss [5,23–26]. However, the sintering temperature range of pure $CaSiO_3$ ceramic is relatively narrow. Chakradhar et al. pointed out that it was difficult to obtain dense $CaSiO_3$ ceramic since its grains grew exceptionally and the bulk $CaSiO_3$ ceramic became more porous with the increase of the calcination temperature [27]. In our previous work, the sintering behavior and microwave dielectric properties of $CaSiO_3$ ceramics have been investigated by a traditional solid-state process and a sol–gel method, respectively [28]. The maximum bulk density of $CaSiO_3$ ceramic sintered at 1340 °C prepared by the conventional

*Corresponding author. Tel.: +86 571 86835781; fax: +86 571 28889527.
E-mail address: sxucjlu@hotmail.com (S. Xu).

0272-8842/$ - see front matter
http://dx.doi.org/10.1016/j.ceramint.2013.09.101

solid-state process is 2.439 g/cm^3, and the microwave dielectric properties are $\varepsilon_r = 6.59$ and $Q \times f = 13{,}109$ GHz. Whereas for $CaSiO_3$ ceramic obtained by the sol–gel method, the maximum bulk density is 2.505 g/cm^3 and the microwave dielectric properties are $\varepsilon_r = 6.69$ and $Q \times f = 25{,}398$ GHz. The density value of the above two samples synthesized either by the traditional solid-state method or by the sol–gel method is much smaller than that of the theoretical density of the $CaSiO_3$ ceramic, which is 2.91 g/cm^3, indicating that it is difficult to obtain dense $CaSiO_3$ ceramic.

In order to improve the sintering characteristics and microwave dielectric properties, Sun and co-workers have used Mg^{2+} to substitute Ca^{2+} in the $CaSiO_3$ host to prepare the CaO–MgO–SiO_2 ceramics for low temperature co-fired ceramic (LTCC) applications [29,30], and $CaMgSi_2O_6$ ceramic has been demonstrated as a potential candidate material for high-frequency devices fabrication [30–32]. The neat $CaMgSi_2O_6$ ceramic sintered at 1290 °C possesses good microwave dielectric properties, e.g. ε_r, $Q \times f$ and τ_f are 7.46, 59,638 GHz and −46 ppm/°C, respectively [30]. However, the sintering temperature range of neat $CaMgSi_2O_6$ ceramic is relatively narrow. In order to improve the sintering property, Zhang and co-workers have used Zn^{2+} to substitute Mg^{2+} in the $CaMgSi_2O_6$ host and found that it was limited to broaden the densification temperature range, although Zn^{2+} substitution for Mg^{2+} could lower the sintering temperature [33].

In this work, we studied a new microwave dielectric ceramic system of $Ca(Mg,Al)(Si,Al)_2O_6$ with low permittivity and low loss. In order to broaden the range of the sintering temperature, Al^{3+} was used to substitute Mg^{2+} and Si^{4+} in the $Ca(Mg_{1-x}Al_x)(Si_{1-x/2}Al_{x/2})_2O_6$ ceramics, and the solid solubility, sintering behavior, microstructure and microwave dielectric properties of this system were investigated.

2. Experimental procedures

Specimen powders were prepared by a conventional solid-state method using high-purity oxide powders (99.99%) of $CaCO_3$, MgO, SiO_2 and Al_2O_3 as raw materials. Stoichiometric proportions of the above powders according to the composition of $Ca(Mg_{1-x}Al_x)(Si_{1-x/2}Al_{x/2})_2O_6$ ($x = 0.01$, 0.02, 0.04, 0.06, 0.08, 0.1, 0.15, 0.2, 0.25, and 0.3) were mixed in ethanol for 24 h with zirconia balls as milling media. The wet mixtures were dried and calcined at 1150–1250 °C for 2 h in air to obtain the $Ca(Mg,Al)(Si,Al)_2O_6$ phase. The calcined powders were re-mixed. After drying and sieving, the as-prepared powders together with the organic binder (5 wt % polyvinyl alcohol) were uniaxially pressed under a pressure of 135 MPa into cylinders of 15 mm in diameter and 8 mm in thickness. These samples were then sintered in the temperature range of 1225–1300 °C for 2 h in air with a heating rate of 5 °C/min.

The bulk densities of the sintered pellets were measured by the Archimedes method using distilled water as medium. The sintered bulks were broken up and ground to powders using an agate mortar. Crystal structures of the powders were performed by the X-ray diffraction (XRD, ARL XTRA) with a Cu K_α radiation (36 kV, 30 mA, and $2\theta = 10$–80°). The polished surfaces of the ceramics were investigated by scanning electron microscopy (SEM, TM3000) after thermal etching. The dielectric constants ε_r and the quality values $Q \times f$ at microwave frequencies were measured by the Hakki–Coleman dielectric resonator method using an Agilent 8719ET (50 MHz to 13.5 GHz) Network Analyzer [34,35]. The temperature coefficient of the resonant frequency τ_f was also measured by the same method in the temperature range from 25 °C to 80 °C and calculated by the following equation:

$$\tau_f = \frac{f_{80} - f_{25}}{f_{25} \times 55} \times 10^6 \ (\text{ppm}/^\circ\text{C})$$

where f_{80} and f_{25} represent the resonant frequency at 80 °C and 25 °C, respectively.

3. Results and discussion

In order to examine the chemical properties of the calcined $Ca(Mg_{1-x}Al_x)(Si_{1-x/2}Al_{x/2})_2O_6$ powders and select a suitable calcining temperature, the starting materials were prepared at 1150, 1175, 1200, 1225 and 1250 °C. Fig. 1 shows the X-ray diffraction patterns of $Ca(Mg_{0.92}Al_{0.08})(Si_{0.96}Al_{0.04})_2O_6$ powders calcined at different temperatures for 2 h. The phases existing at each calcining temperature are observed, as illustrated in this figure. It can be seen clearly that the phases of $CaSiO_3$ (PDF 27-0088), $Ca_2MgSi_2O_7$ (PDF 35-0592), MgO (PDF 45-0946) and SiO_2 (PDF 27-0605) are present at the calcining temperature of 1150 °C, accompanied by a small amount of $Ca(Mg,Al)(Si,Al)_2O_6$ (PDF 41-1370). When the calcining temperature is increased from 1150 °C to 1200 °C, the mixed powders react more and the intensity of major $Ca(Mg,Al)(Si,Al)_2O_6$ phase is enhanced, whereas those of $CaSiO_3$, $Ca_2MgSi_2O_7$, MgO and SiO_2 are weakened. Homogeneous $Ca(Mg,Al)(Si,Al)_2O_6$ phase with diopside structure can be obtained at about 1225–1250 °C. So 1225 °C was selected as the calcining temperature.

The crystalline phases in $Ca(Mg_{1-x}Al_x)(Si_{1-x/2}Al_{x/2})_2O_6$ ceramics with different x values sintered at 1250 °C for 2 h were identified and the XRD diffraction patterns are showed in

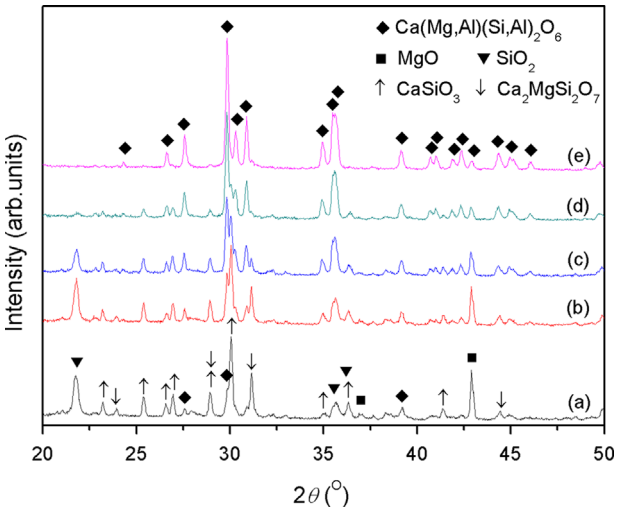

Fig. 1. XRD patterns of $Ca(Mg_{0.92}Al_{0.08})(Si_{0.96}Al_{0.04})_2O_6$ powders calcined at (a) 1150 °C, (b) 1175 °C, (c) 1200 °C, (d) 1225 °C and (e) 1250 °C.

Fig. 2. As the x value is increased from 0.02 to 0.15, the patterns are similar and match well with $Ca(Mg,Al)(Si,Al)_2O_6$ (PDF 41-1370), and all of the peaks are indexed without any secondary phases. However, a second phase of $CaAl_2SiO_6$ (PDF 31-0249) is observed when the x value reaches 0.2, and the intensity of the second phase peaks increases with the increase of the x value. These results suggest that the solubility limit of Al_2O_3 in $Ca(Mg,Al)(Si,Al)_2O_6$ is between 0.15 and 0.2. $Ca(Mg,Al)(Si,Al)_2O_6$ is a chain silicate, crystallizing in monoclinic symmetry with a space group of C2/c, where $a=9.732$ Å, $b=8.867$ Å, $c=5.279$ Å, $\alpha=\gamma=90^\circ$ and $\beta=106.29^\circ$ (PDF 41-1370). Fig. 3 presents the structure of $Ca(Mg,Al)(Si,Al)_2O_6$. The ionic radii of Mg^{2+}, Si^{4+} and Al^{3+} are 0.72 Å, 0.40 Å and 0.535 Å, respectively. Based on the equation of $\Delta r=(r_A-r_B)/r_A$, the Δr between Mg^{2+} and Al^{3+} is 25.69%, and that between Si^{4+} and Al^{3+} is 33.75%. These large ionic radii difference results in the limited Al^{3+} substitution for Mg^{2+} and Si^{4+}.

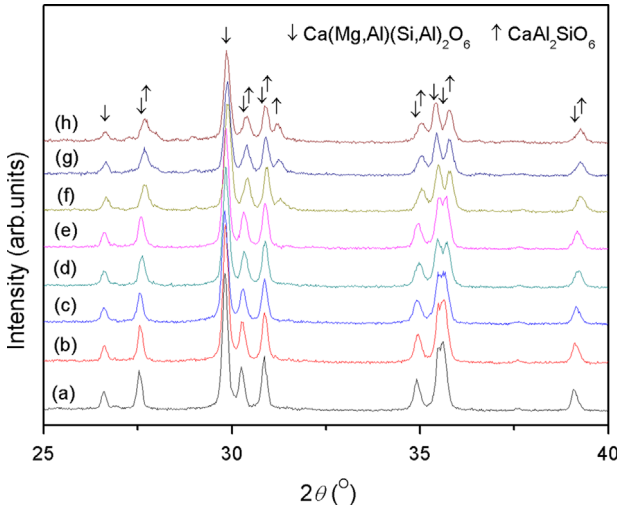

Fig. 2. XRD patterns of $Ca(Mg_{1-x}Al_x)(Si_{1-x/2}Al_{x/2})_2O_6$ ceramics sintered at 1250 °C with x value of (a) 0.02, (b) 0.04, (c) 0.08, (d) 0.1, (e) 0.15, (f) 0.2, (g) 0.25 and (h) 0.3.

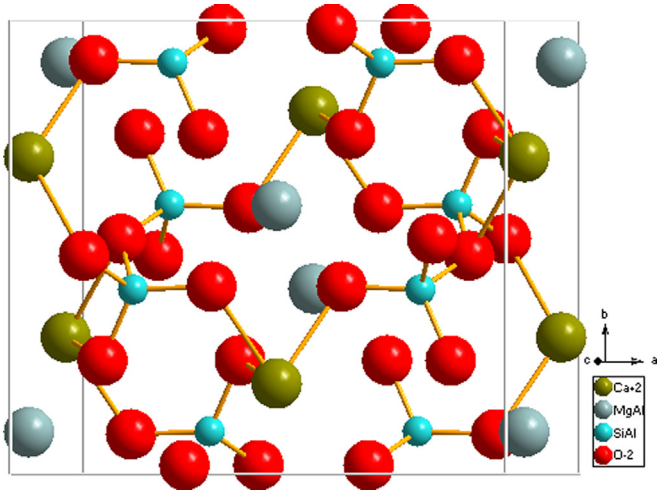

Fig. 3. The structure of $Ca(Mg,Al)(Si,Al)_2O_6$.

Fig. 4 shows the bulk densities of $Ca(Mg_{1-x}Al_x)(Si_{1-x/2}Al_{x/2})_2O_6$ ceramics sintered at different temperatures. The densification temperatures can be extracted from the plots in this figure. Densification temperatures of 1300 °C, 1275 °C and 1250 °C are obtained for the compositions of $x=0.01$–0.02, $x=0.04$–0.1 and $x=0.1$–0.15, respectively. Sintered at 1250 °C, the figure shows that the bulk density increases with the increase of the x value from 0.01 to 0.15. These results indicate that the Al^{3+} substitution can promote the sintering process and lower the densification temperature of $Ca(Mg,Al)(Si,Al)_2O_6$ ceramics. For the compositions of $x=0.08$–0.15, a broadened densification temperature range of 1250–1300 °C is observed. It is also seen from the figure that the bulk density of $Ca(Mg_{1-x}Al_x)(Si_{1-x/2}Al_{x/2})_2O_6$ ceramics sintered at 1250 °C decreases with the increase of the x value from 0.15 to 0.3. The $CaAl_2SiO_6$ second phase occurs as the x value reaches 0.2 (shown in Fig. 2). Therefore, it is considered that the bulk density of $CaAl_2SiO_6$ ceramic is lower than that of $Ca(Mg,Al)(Si,Al)_2O_6$ ceramic. Meanwhile, we have found that the pellets melted when sintered at 1275 °C for the compositions of $x=0.25$–0.3 and sintered at 1300 °C for the compositions of $x=0.2$–0.3, indicating that the melt point of $CaAl_2SiO_6$ is about 1250–1275 °C.

The microstructures of $Ca(Mg_{1-x}Al_x)(Si_{1-x/2}Al_{x/2})_2O_6$ ceramics sintered at 1250 °C with different x values are presented in Fig. 5(a)–(f). Fig. 5(a) shows that the average grain size is about 1 μm and there are many pores in the bulks, which indicates that $Ca(Mg_{1-x}Al_x)(Si_{1-x/2}Al_{x/2})_2O_6$ ceramic with the x value of 0.02 can be hardly sintered at 1250 °C. With the increase of the x value to 0.06, the size of the grains grows and the porosity decreases, as shown in Fig. 5(b). When the x value increases sequentially to 0.08–0.10, the specimens become well-densified as well as rapid grain growth. It indicates that appropriate Al^{3+} substitution ($x=0.08$–0.10) can promote the sintering process of $Ca(Mg,Al)(Si,Al)_2O_6$ ceramics, which is consistent with the results of the bulk densities sintered at different temperatures, as shown in Fig. 4.

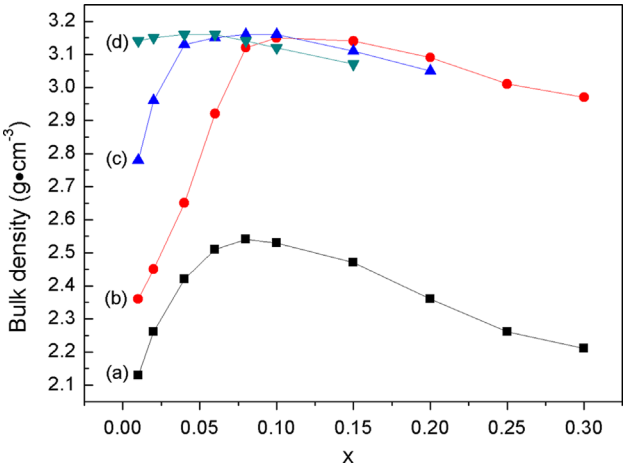

Fig. 4. Bulk densities of $Ca(Mg_{1-x}Al_x)(Si_{1-x/2}Al_{x/2})_2O_6$ ceramics with different x values sintered at (a) 1225 °C, (b) 1250 °C, (c) 1275 °C and (d) 1300 °C.

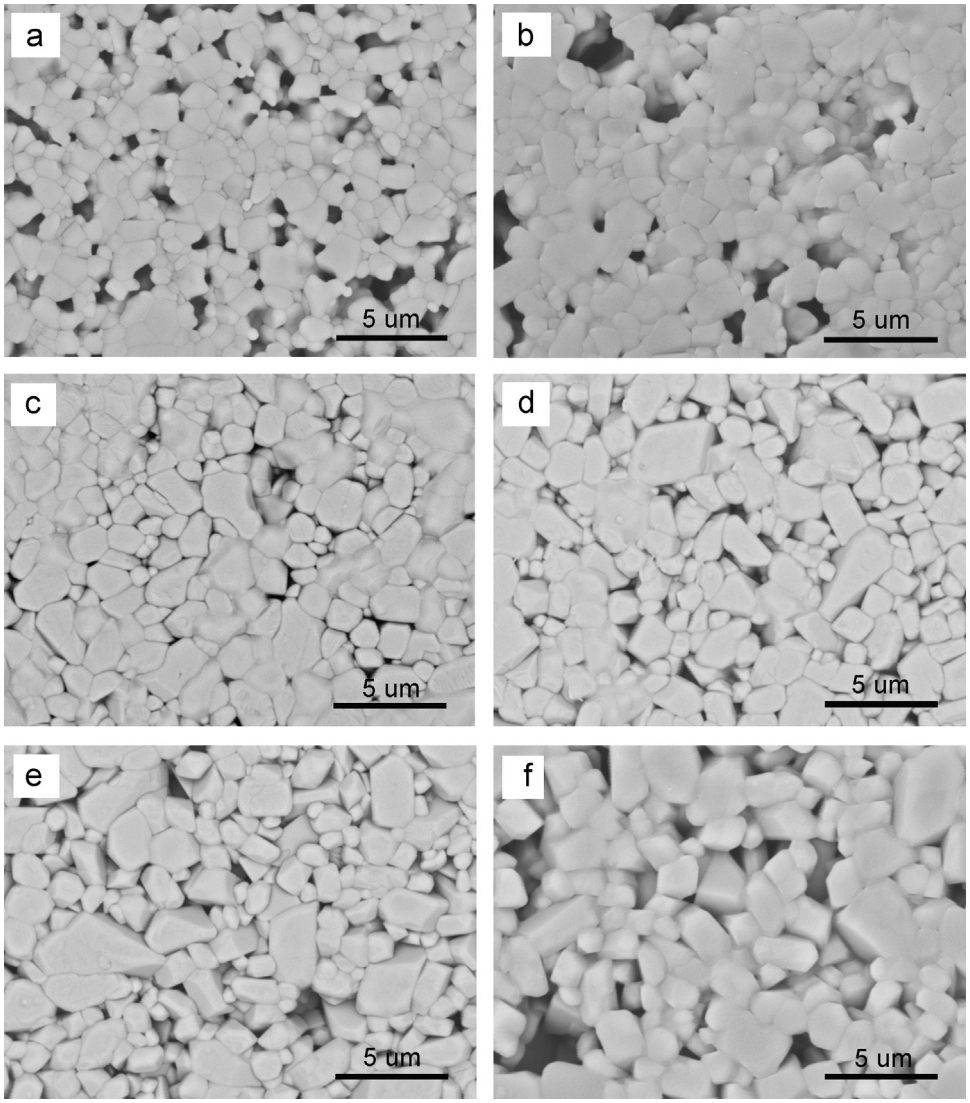

Fig. 5. SEM photographs of $Ca(Mg_{1-x}Al_x)(Si_{1-x/2}Al_{x/2})_2O_6$ ceramics sintered at 1250 °C with x value of (a) 0.02, (b) 0.06, (c) 0.08, (d) 0.1, (e) 0.15 and (f) 0.2.

However, the surface of the ceramics seems to be porous as the x value reaches 0.2. One possible explanation is that the volatilization of the $CaAl_2SiO_6$ second phase occurs during thermal etching and results in porosity.

Fig. 6 shows the images of thermally etched surfaces of $Ca(Mg_{1-x}Al_x)(Si_{1-x/2}Al_{x/2})_2O_6$ ceramics sintered at their optimum temperatures with different x values. The evident equiaxed grain morphology is observed for $x=0.01$–0.02, while a certain number of columnar grain morphology is observed for the ceramics with $x=0.08$–0.15. Lattice constants such as $a=9.733$ Å, $b=8.909$ Å, and $c=5.296$ Å for $Ca(Mg_{0.7}Al_{0.3})(Si_{0.85}Al_{0.15})_2O_6$ (ICSD 158207) and $a=9.697$ Å, $b=8.850$ Å, and $c=5.306$ Å for $Ca(Mg_{0.5}Al_{0.5})(Si_{0.75}Al_{0.25})_2O_6$ (ICSD 158208) can be extracted from the XRD patterns, which indicates that the lattice parameter in the c-axis increases with the Al^{3+} substitution, while those in the a- and b-axes decrease. Moreover, the lattice parameter in the c-axis is much smaller than those in the a- and b-axes. So the growth rate of crystal is faster for the c-axis direction than that for the a- and b-axes with Al^{3+} substitution [36,37], which results in columnar grain morphology for $Ca(Mg_{1-x}Al_x)(Si_{1-x/2}Al_{x/2})_2O_6$ ceramics with high x values.

Microwave dielectric properties of $Ca(Mg_{1-x}Al_x)(Si_{1-x/2}Al_{x/2})_2O_6$ ceramics sintered at the optimum temperatures as a function of the x value are illustrated in Table 1 and Fig. 7. The dielectric constant (ε_r) increases roughly linearly from 7.79 to 7.95 as the x value increases from 0.01 to 0.15, indicating the Al^{3+} substitution can promote the apparent improvement of the dielectric constant of the $Ca(Mg,Al)(Si,Al)_2O_6$ ceramics. Further increase of the x value leads to the increase of the ε_r eventually to 8.16 for the composition of $x=0.3$. As shown in the XRD patterns (Fig. 2), the solubility limit of Al_2O_3 in $Ca(Mg,Al)(Si,Al)_2O_6$ is between 0.15 and 0.2, and $CaAl_2SiO_6$ second phase occurs as the x value reaches 0.2. Combined with the empirical rule of $\ln \varepsilon_r = \sum_i V_i \ln \varepsilon_{ri}$, where V_i and ε_{ri} are the volume fraction and the permittivity of each phase, respectively [38], we conclude that the dielectric constant of the $CaAl_2SiO_6$ second phase is larger than that of $Ca(Mg,Al)(Si,Al)_2O_6$ ceramic.

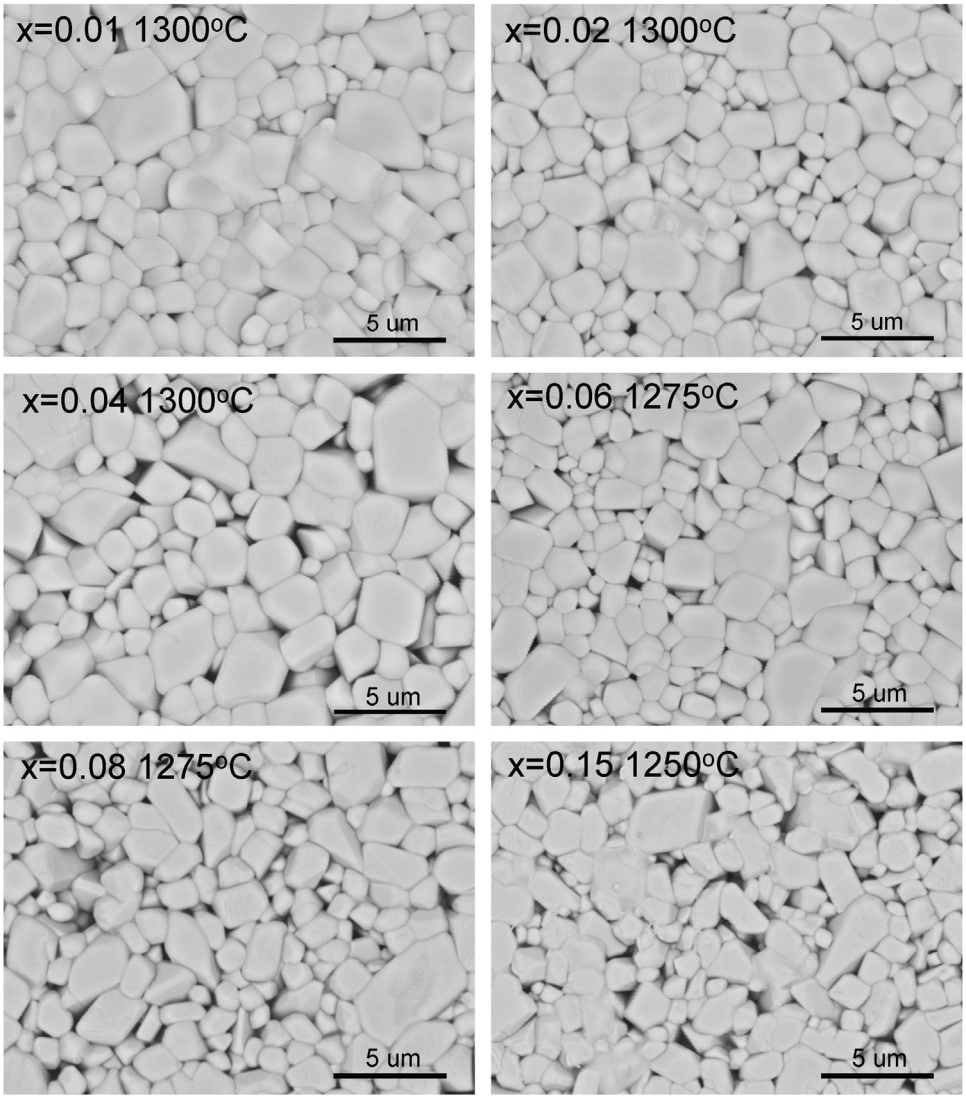

Fig. 6. SEM photographs of $Ca(Mg_{1-x}Al_x)(Si_{1-x/2}Al_{x/2})_2O_6$ ceramics sintered at the optimum temperature with various compositions.

The $Q \times f$ values of the well-sintered $Ca(Mg_{1-x}Al_x)(Si_{1-x/2}Al_{x/2})_2O_6$ ceramics increase from 57,322 GHz to 59,772 GHz as the x value increases from 0.01 to 0.08, and then they are saturated in the range of $x=0.08$–0.2. As the x value reaches 0.3, the $Q \times f$ value decreases dramatically to 43,727 GHz. It was reported that the microwave dielectric loss was mainly caused not only by the lattice vibrational modes, but also by the pores, the grain morphology and the secondary phases. As shown in Fig. 5, high x value ($x=0.2$) results in porosity. In addition, the $CaAl_2SiO_6$ second phase occurs as the x value exceeds 0.2. So the $Q \times f$ value decreases with the increase of the x value in the composition range of 0.2–0.3. Combined with the sintering behavior, good microwave dielectric properties of $\varepsilon_r=7.89$ and $Q \times f=59{,}772$ GHz were obtained for the ceramics with the composition of $x=0.08$ sintered at 1275 °C, which possesses a broadened densification temperature range of 1250–1300 °C.

From the temperature coefficient of frequency (τ_f) of well-sintered $Ca(Mg_{1-x}Al_x)(Si_{1-x/2}Al_{x/2})_2O_6$ ceramics with the composition range of 0.01–0.3, it is clear that the τ_f values range from −39.42 to −44.92 ppm/°C and show a rising trend with the increase of the x value. The τ_f is well known to be governed by the composition, the additives and the second phase of the materials. The increase of the τ_f value with the x value increasing may have been caused by the change in the volume of the crystal unit cell. Moreover, it is considered that the τ_f value of $CaAl_2SiO_6$ second phase is lower than that of $Ca(Mg,Al)(Si,Al)_2O_6$ ceramics. In general, because a near-zero τ_f value of dielectric ceramics is necessary for commercial applications, an improvement in τ_f value, closer to 0 ppm/°C, is required in this system.

4. Conclusions

The crystalline phases of $Ca(Mg_{1-x}Al_x)(Si_{1-x/2}Al_{x/2})_2O_6$ ceramics ($x=0.01$–0.3) showed that the solubility limit of Al_2O_3 in $Ca(Mg,Al)(Si,Al)_2O_6$ was between 0.15 and 0.2, and a second phase of $CaAl_2SiO_6$ was obtained as the x value reached 0.2. Appropriate Al^{3+} substitution for Mg^{2+} and Si^{4+}

Table 1
Microwave dielectric properties and apparent density of $Ca(Mg_{1-x}Al_x)(Si_{1-x/2}Al_{x/2})_2O_6$ ceramics sintered at the optimum temperature.

$Ca(Mg_{1-x}Al_x)(Si_{1-x/2}Al_{x/2})_2O_6$	Diameter (mm)	Height (mm)	ρ (g cm^{-3})	f_0 (GHz)	ε_r	$Q\times f$ (GHz)	τ_f (ppm/°C)
x=0.01/1300°C	12.45	6.10	3.14	11.26	7.79	57,322	−39.52
x=0.02/1300°C	12.44	6.02	3.15	11.32	7.80	57,470	−39.42
x=0.04/1300°C	12.42	6.06	3.16	11.53	7.84	57,770	−40.01
x=0.06/1275°C	12.49	5.98	3.15	11.33	7.86	57,504	−42.09
x=0.08/1275°C	12.49	6.15	3.16	11.40	7.89	59,772	−42.12
x=0.10/1250°C	12.42	6.01	3.15	11.67	7.92	59,387	−43.28
x=0.15/1250°C	12.44	6.04	3.14	11.54	7.95	59,134	−42.68
x=0.20/1250°C	12.47	6.02	3.09	11.31	8.02	60,203	−44.18
x=0.25/1250°C	12.76	5.99	3.01	11.06	8.11	55,734	−43.85
x=0.30/1250°C	12.82	6.12	2.97	10.89	8.16	43,727	−44.92

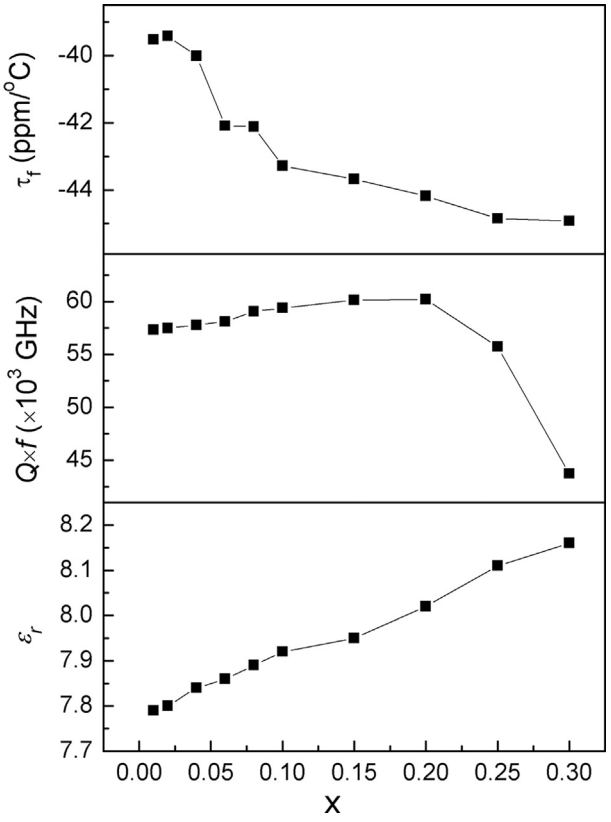

Fig. 7. Microwave dielectric properties of $Ca(Mg_{1-x}Al_x)(Si_{1-x/2}Al_{x/2})_2O_6$ ceramics sintered at the optimum temperature as a function of the composition x.

could promote the sintering process and lower the densification temperature of $Ca(Mg_{1-x}Al_x)(Si_{1-x/2}Al_{x/2})_2O_6$ ceramics. The densification temperatures were 1300 °C, 1275 °C and 1250 °C for the compositions of x=0.01–0.02, x=0.04–0.08 and x=0.1–0.3, respectively. Meanwhile, a broadened densification temperature range of 1250–1300 °C was obtained for the compositions of x=0.08–0.15. With the x value increase from 0.01 to 0.3, the dielectric constant (ε_r) increased roughly linearly from 7.79 to 8.16, and the temperature coefficient of frequency (τ_f) showed a rising trend ranging from −39.42 to −44.92 ppm/°C. The $Q\times f$ values increased from 57,322 GHz to 59,772 GHz as the x value increased from 0.01 to 0.08, and then they were saturated in the range of x=0.08–0.2. However, further increase of the x value ($x\geq 0.25$) deteriorated the microwave dielectric properties. Combined with the sintering behavior, good microwave dielectric properties of ε_r=7.89, $Q\times f$=59,772 GHz and τ_f= −42.12 ppm/°C were obtained for the ceramics with the composition of x=0.08 sintered at 1275 °C.

Acknowledgments

This work was financially supported by the Science and Technology Innovative Research Team of Zhejiang Province (2010R50016) and the Nature Science Foundation of Zhejiang Province (Y1110648).

References

[1] S.S. Rajput, S. Keshri, V.R. Gupta, N. Gupta, V. Bovtun, J. Petzelt, Design of microwave dielectric resonator antenna using MZTO–CSTO composite, Ceramics International 38 (2012) 2355–2362.
[2] M.N. Suma, P.V. Bijumon, M.T. Sebastian, P. Mohanan, A compact hybrid CPW fed planar monopole/dielectric resonator antenna, Journal of the European Ceramic Society 27 (2007) 3001–3004.
[3] S. Parida, S.K. Rout, V. Subramanian, P.K. Barhai, N. Gupta, V. R. Gupta, Structural, microwave dielectric properties and dielectric resonator antenna studies of $Sr(Zr_xTi_{1-x})O_3$ ceramics, Journal of Alloys and Compounds 528 (2012) 126–134.
[4] Y.C. Chen, K.C. Chang, D.Y. Tsai, A hybrid dielectric resonator antenna based upon novel complex perovskite microwave ceramic, Ceramics International 39 (2013) 8043–8048.
[5] J.S. Kim, M.E. Song, M.R. Joung, J.H. Choi, S. Nahm, S.I. Gu, J.H. Paik, B.H. Choi, Effect of B_2O_3 addition on the sintering temperature and microwave dielectric properties of Zn_2SiO_4 ceramics, Journal of the European Ceramic Society 30 (2010) 375–379.
[6] C. Jiang, S.P. Wu, Q. Ma, Y.X. Mei, Synthesis and microwave dielectric properties of Nd_2SiO_5, Journal of Alloys and Compounds 544 (2012) 141–144.
[7] M. Ohashi, H. Ogawa, A. Kan, E. Tanaka, Microwave dielectric properties of low-temperature sintered $Li_3AlB_2O_6$ ceramic, Journal of the European Ceramic Society 25 (2005) 2877–2881.
[8] A. Belous, O. Ovchar, D. Durilin, M.M. Krzmanc, M. Valant, D. Suvorov, High-Q microwave dielectric materials based on the spinel Mg_2TiO_4, Journal of the American Ceramic Society 89 (2006) 3441–3445.
[9] C.W. Zheng, S.Y. Wu, X.M. Chen, K.X. Song, Modification of $MgAl_2O_4$ microwave dielectric ceramics by Zn substitution, Journal of the American Ceramic Society 90 (2007) 1483–1486.

[10] W. Lei, W.Z. Lu, X.C. Wang, Temperature compensating $ZnAl_2O_4$–Co_2TiO_4 spinel-based low-permittivity microwave dielectric ceramics, Ceramics International 38 (2012) 99–103.
[11] R.C. Pullar, S. Farrah, N.M. Alford, $MgWO_4$, $ZnWO_4$, $NiWO_4$ and $CoWO_4$ microwave dielectric ceramics, Journal of the European Ceramic Society 27 (2007) 1059–1063.
[12] D. Zhou, C.A. Randall, L.X. Pang, H. Wang, J. Guo, G.Q. Zhang, X. G. Wu, L. Shui, X. Yao, Microwave dielectric properties of Li_2WO_4 ceramic with ultra-low sintering temperature, Journal of the American Ceramic Society 94 (2011) 348–350.
[13] E.S. Kim, S.H. Kim, B.I. Lee, Low-temperature sintering and microwave dielectric properties of $CaWO_4$ ceramics for LTCC applications, Journal of the European Ceramic Society 26 (2006) 2101–2104.
[14] S.F. Wang, Y.R. Wang, Y.F. Hsu, H.C. Lu, J.S. Tsai, Ultra-low-fire $Te_2(Mo_{1-x}W_x)O_7$ ceramics: microstructure and microwave dielectric properties, Journal of the American Ceramic Society 93 (2010) 4071–4074.
[15] D. Zhou, C.A. Randall, L.X. Pang, H. Wang, X.G. Wu, J. Guo, G. Q. Zhang, L. Shui, X. Yao, Microwave dielectric properties of $Li_2(M^{2+})_2Mo_3O_{12}$ and $Li_3(M^{3+})Mo_3O_{12}$(M=Zn, Ca, Al, In) lyonsite-related-type ceramics with ultra-low sintering temperatures, Journal of the American Ceramic Society 94 (2011) 802–805.
[16] R. Umemura, H. Ogawa, H. Ohsato, A. Kan, A. Yokoi, Microwave dielectric properties of low-temperature sintered $Mg_3(VO_4)_2$ ceramic, Journal of the European Ceramic Society 25 (2005) 2865–2870.
[17] R. Umemura, H. Ogawa, A. Yokoi, H. Ohsato, A. Kan, Low-temperature sintering-microwave dielectric property relations in $Ba_3(VO_4)_2$ ceramic, Journal of Alloys and Compounds 424 (2006) 388–393.
[18] A. Kan, H. Ogawa, A. Yokoi, Sintering temperature dependence of microwave dielectric properties in $Mg_4(TaNb_{1-x}V_x)O_9$ compounds, Materials Research Bulletin 41 (2006) 1178–1184.
[19] Y.M. Ding, J.J. Bian, Sintering behavior and microwave dielectric properties of $Ca_{1-x}Bi_xW_{1-x}V_xO_4$ ceramics, Ceramics International 39 (2013) 1555–1560.
[20] J.J. Bian, D.W. Kim, K.S. Hong, Glass-free LTCC microwave dielectric ceramics, Materials Research Bulletin 40 (2005) 2120–2129.
[21] T. Guo, W.J. Wu, Y.L. Wang, Y.X. Li, Relations on synthesis, crystal structure and microwave dielectric properties of $SrZnP_2O_7$ ceramics, Ceramics International 38 (2012) S187–190.
[22] K. Mori, H. Ogawa, A. Kan, H. Ohsato, Microwave dielectric property-microstructure relationships in $Y_2Ba(Cu_{1-x}Mg_x)O_5$ solid solutions, Journal of the European Ceramic Society 24 (2004) 1749–1753.
[23] L. Cheng, P. Liu, X.M. Chen, W.C. Niu, G.G. Yao, C. Liu, X.G. Zhao, Q. Liu, H.W. Zhang, Fabrication of nanopowders by high energy ball milling and low temperature sintering of Mg_2SiO_4 microwave dielectrics, Journal of Alloys and Compounds 513 (2012) 373–377.
[24] K.X. Song, X.M. Chen, C.W. Zheng, Microwave dielectric characteristics of ceramics in Mg_2SiO_4–Zn_2SiO_4 system, Ceramics International 34 (2008) 917–920.
[25] J.L. Zou, Q.L. Zhang, H. Yang, H.P. Sun, A new system of low temperature sintering ZnO–SiO_2 dielectric ceramics, Japanese Journal of Applied Physics 45 (2006) 4143–4145.
[26] H.P. Wang, J.M. Chen, W.Y. Yang, S.Q. Feng, H.P. Ma, G.H. Jia, S. Q. Xu, Effects of Al_2O_3 addition on the sintering behavior and microwave dielectric properties of $CaSiO_3$ ceramics, Journal of the European Ceramic Society 32 (2012) 541–545.
[27] R.P.S. Chakradhar, B.M. Nagabhushana, G.T. Chandrappa, K.P. Ramesh, J.L. Rao, Solution combustion derived nanocrystalline macroporous wollastonite ceramics, Materials Chemistry and Physics 95 (2006) 169–175.
[28] H.P. Wang, Q.L. Zhang, H. Yang, H.P. Sun, Synthesis and microwave dielectric properties of $CaSiO_3$ nanopowder by the sol–gel process, Ceramics International 34 (2008) 1405–1408.
[29] Q.L. Zhang, H. Yang, H.P. Sun, A new microwave ceramic with low-permittivity for LTCC applications, Journal of the European Ceramic Society 28 (2008) 605–609.
[30] H.P. Sun, Q.L. Zhang, H. Yang, J.L. Zou, $(Ca_{1-x}Mg_x)SiO_3$: a low-permittivity microwave dielectric ceramic system, Materials Science and Engineering: B 138 (2007) 46–50.
[31] T. Joseph, M.T. Sebastian, H. Sreemoolanadhan, V.K.S. Nageswari, Effect of glass addition on the microwave dielectric properties of $CaMgSi_2O_6$ Ceramics, International Journal of Applied Ceramic Technology 7 (2010) E98–106.
[32] H.P. Wang, S.Q. Xu, S.Y. Zhai, D.G. Deng, H.D. Ju, Effect of B_2O_3 additives on the sintering and dielectric behaviors of $CaMgSi_2O_6$ ceramics, Journal of Materials Science and Technology 26 (2010) 351–354.
[33] J. Zhang, Y.Y. Zhou, Z.X. Yuen, Low-temperature sintering and microwave dielectric properties of LiF-doped $CaMg_{1-x}Zn_xSi_2O_6$ ceramics, Ceramics International 39 (2013) 2051–2508.
[34] B.W. Hakki, P.D. Coleman, A dielectric resonator method of measuring inductive capacitors in the millimeter range, IEEE Transactions Microwave Theory and Techniques 8 (1960) 402–410.
[35] W.E. Courtey, Analysis and evaluation of a method of measuring the complex permittivity and permeability microwave insulators, IEEE Transactions Microwave Theory and Techniques 18 (1970) 475–485.
[36] K. Wada, K. Kakimoto, H. Ohsato, Microstructure and microwave dielectric properties of $Ba_4Sm_{9.33}Ti_{18}O_{54}$ ceramics containing columnar crystals, Journal of the European Ceramic Society 23 (2003) 2535–2539.
[37] L. Zhong, X.L. Zhu, X.M. Chen, X.Q. Liu, L. Li, Solubility limits and microwave dielectric properties of $Ba_{6-3x}Sm_{8+2x}Ti_{18}O_{54}$ solid solution, Ceramics International 37 (2011) 3575–3581.
[38] C.L. Huang, S.S. Liu, C.C. Chen, High dielectric constant low loss in the $(La_{1/2}Na_{1/2})TiO_3$–$Ca(Mg_{1/3}Nb_{2/3})O_3$ ceramic system at microwave frequency, Journal of Alloys and Compounds 468 (2009) L13–16.